J Math Chem (2008) 44:142–171
DOI 10.1007/s10910-007-9298-7

ORIGINAL PAPER

Principles for determining mechanistic pathways from observable quantum control data

Richard Sharp · Abhra Mitra · Herschel Rabitz

Received: 21 February 2007 / Accepted: 14 May 2007 / Published online: 21 September 2007

Abstract Hamiltonian encoding (HE) methods have been used to understand mechanism in computational studies of laser controlled quantum systems. This work studies the principles for extending such methods to extract control mechanisms from laboratory data. In an experimental setting, observables replace the utilization of wavefunctions in computational HE. With laboratory data, HE gives rise to a set of quadratic equations for the interfering transition amplitudes, and the solution to the equations reveals the mechanistic pathways. The extraction of the mechanism from the system of quadratic equations raises questions of uniqueness and solvability, even in the ideal case without noise. Symmetries are shown to exist in the quadratic system of equations, which is generally overdetermined. Therefore, the mechanism is likely to be unique up to these symmetries. Numerical simulations demonstrate the concepts on simple model systems.

Keywords Schrödinger equation · quantum control · control mechanism · Hamiltonian Encoding · quantum theory

1 Introduction

The control of quantum mechanical systems is a growing area of research, which is being explored for fundamental reasons as well as for many potential applications. Optimal control by closed-loop procedures [1,2] is a general technique which is being used to find effective fields in a number of experimental contexts [3–10]. However,

R. Sharp
Mathematical Sciences, Carnegia Mellon University, Pittsburgh, PA 15213, USA

A. Mitra · H. Rabitz(✉)
Department of Chemistry, Princeton University, Princeton, NJ 08544, USA
e-mail: hrabitz@princeton.edu

achieving control generally does not reveal the mechanism of the controlled dynamics, either from an optimal or suboptimal field. Even in computer simulations, which exploit full knowledge of the wavefunction, the mechanism by which a control field achieves its target is often hidden, almost regardless of how the control field is deduced.

Hamiltonian encoding (HE) was originally proposed as a technique for understanding mechanism in the context of computer simulations [11,12]. The ultimate goal of HE is to directly reveal mechanism in the laboratory, and initial simulations [13] show that such a procedure is feasible. There are a number of challenges in considering laboratory based HE. These issues may be classified as either fundamental (e.g., solving the equations produced by the encoding process) or practical (e.g., operating with the presence of noise in the control and measurements). This work studies the fundamental aspects of laboratory based HE, given an ideal experimental setup, although some practical issues are also addressed. By working in the ideal limit, the fundamental procedure for extracting mechanism can be assessed; dealing with imperfections such as control noise and data errors must build upon this foundation. Any practical application of HE will necessarily involve at least some physical knowledge of the specific system under investigation. Such information has the potential to simplify mechanism extraction. For example, a priori knowledge of forbidden transitions can reduce the system of equations arising in HE mechanism analysis. However, the form of such specific knowledge may vary widely. We will not rely on such knowledge in this work, but we will indicate in some examples how such information may benefit mechanism analysis.

HE defines mechanism in terms of interaction integrals (also referred to as pathway amplitudes) arising from a series expansion of the time evolution operator, $U(t)$. These integrals can be difficult to compute by traditional means and cannot be directly observed in the laboratory. Earlier work [11,12] on HE described a method to computationally extract these pathway amplitudes. In a computational setting, given the control field, the Schrödinger equation can be integrated to obtain $U(T)$ at the final time T. A family of Hamiltonians $H(s)$ is generated with controls parametrized by the variable $s \geq 0$, such that these encoded Hamiltonians are systematically linked to the original Hamiltonian $H(0)$. The set of Schrödinger equations driven by this family of encoded Hamiltonians is solved to generate $U(T, s)$. The mechanism, which underlies $U(T) = U(T, 0)$, is extracted from scanning the s dependence of $U(T, s)$.

In the laboratory, control experiments operate using observable information, rather than direct access to the wavefunction. For example, closed-loop control is typically conducted in the laboratory to maximize a target observable $\langle O \rangle$ at a final time T. Laboratory based HE has been proposed [14], to operate with similar logic to its computational counterpart, except that the solution to Schrödinger's equation is provided experimentally, not computationally. In the laboratory, once an effective control field $\mathcal{E}(t)$ has been identified, a family of encoded control fields $\mathcal{E}(t, s)$, $s \geq 0$ parametrized by s would be generated with the constraint $\mathcal{E}(t, s = 0) \equiv \mathcal{E}(t)$. The variation in the target observable $\langle O(s) \rangle$ would be monitored as a function of s, and the mechanism information extracted from it. This paper examines the fundamental issues involved when HE is performed using observable information.

The paper is organized as follows. Section 2 is an introduction to HE by field modulation. The representation of the control field and three different modulation

schemes are discussed in Sect. 3. HE associated with observable data entails the solution of a system of quadratic equations. This paper addresses the formulation of these equations and their solution. Section 4 discusses the general solvability of the system of equations arising from HE. One condition for a unique solution, considering that a solution must exist by virtue of the problem's physical basis, is that the system be overdetermined. Overdetermined systems of equations are shown to be the typical case for HE in Sect. 5. An explicit example of the procedure is presented in Sects. 6, and 7 considers several algorithmic approaches useful in specific cases of HE. Finally, conclusions are given in Sect. 8.

2 Hamiltonian encoding using field modulation

This section summarizes the basic concepts of field based HE introduced in [13] to lay the foundation for the analysis in the subsequent sections. The quantum system interacts with the electric field generated by a shaped laser pulse. Considering a dipole interaction, the Hamiltonian may be written as

$$i\hbar\frac{dU}{\mathrm{d}t} = [H_0 - \mu\mathcal{E}(t)]U \tag{1}$$

where H_0 is the field free Hamiltonian and μ is the dipole operator coupling the system to the control field $\mathcal{E}(t)$. The control goal is to move the system from an initial state $|a\rangle$ at $t = 0$ to a final state $|b\rangle$ at the time $t = T$. The equation of motion for the time evolution operator in the interaction representation is given by

$$i\hbar\frac{dU_I}{\mathrm{d}t} = -\mu_I(t)\mathcal{E}(t)U_I, \tag{2}$$

and for notational simplicity it is understood hereafter that U is in the interaction representation. Consider the element, $U_{ba} = \langle b|U(T)|a\rangle$ corresponding to the transition from state $|a\rangle$ to $|b\rangle$, which can be written in Dyson series form as

$$\begin{aligned} U_{ba} = \langle b|a\rangle &+ \left(\frac{i}{\hbar}\right)\int_0^T \langle b|\mu_I(t_1)\mathcal{E}(t_1)|a\rangle\, dt_1 \\ &+ \left(\frac{i}{\hbar}\right)^2\int_0^T\int_0^{t_2} \langle b|\mu_I(t_2)\mathcal{E}(t_2)\mu_I(t_1)\mathcal{E}(t_1)|a\rangle\, dt_1\, dt_2 \\ &+ \cdots . \end{aligned} \tag{3}$$

While this expansion is an infinite series, we shall truncate it at some order, N, under the assumption that terms of order $N + 1$ and beyond are negligible. The control field can also be decomposed, using the basis functions $\epsilon_m(t)$

$$\mathcal{E}(t) = \sum_{m=1}^{\infty} c_m\epsilon_m(t). \tag{4}$$

In any practical setting, and in the remainder of this paper, the expansion of the electric field in Eq. 4 will be truncated at some finite value M. In field based HE, control *pathways* are defined by interactions between the system and components of the control field $\{\epsilon_m(t)\}$. The choice of basis functions or field components, $\epsilon_m(t)$ is, in principle, arbitrary. However, the number of basis functions M needed to represent the control field, and hence the nature and number of pathways, can vary greatly, depending on the choice of basis functions, and certain representations tend to be favored (e.g., a Fourier basis is typically used in the laboratory and is also mathematically convenient). Control mechanism will always be understood in reference to a representation or basis, and field based HE reflects this situation [13,15].

Inserting the expanded electric field of Eq. 4 into Eq. 3 yields

$$\begin{aligned} U_{ba} = \langle b|a\rangle &+ \left(\frac{i}{\hbar}\right)\sum_{m_1=1}^{M}\int_0^T \langle b|\mu_I(t_1)c_{m_1}\epsilon_{m_1}(t_1)|a\rangle dt_1 \\ &+ \left(\frac{i}{\hbar}\right)^2\sum_{m_1=1}^{M}\sum_{m_2=1}^{M}\int_0^T\int_0^{t_2} \langle b|\mu_I(t_2)c_{m_2}\epsilon_{m_2}(t_2)\mu_I(t_1)c_{m_1}\epsilon_{m_1}(t_1)|a\rangle dt_1 dt_2 \\ &+ \cdots . \end{aligned} \tag{5}$$

Each term in Eq. 5 can be interpreted as the complex valued amplitude of a particular transition pathway: the first term is the projection of the initial state onto the final state, the second term is a summation over all M field components $\epsilon_{m_1}(t_1)$ inducing direct transitions from the state $|a\rangle$ to $|b\rangle$. The subsequent terms, such as

$$\left(\frac{i}{\hbar}\right)^n \int_0^T \cdots \int_0^{t_2} \langle b|c_{m_n}\epsilon_{m_n}(t_n)\mu_I(t_n)\ldots c_{m_1}\epsilon_{m_1}(t_1)\mu_I(t_1)|a\rangle dt_1\ldots dt_n, \tag{6}$$

represent higher order transitions induced by multiple interactions with various field components $\epsilon_{m_1}(t_1),\ldots,\epsilon_{m_n}(t_n)$.

HE produces pathways linking $|a\rangle$ and $|b\rangle$ without distinguishing the order in which the field components interact with the system. Therefore the field pathway, denoted $(\epsilon_{m_1},\ldots,\epsilon_{m_n})$, is defined as the sum of all pathways linking $|a\rangle$ to $|b\rangle$ via the field components $\epsilon_{m_1},\ldots,\epsilon_{m_n}$, regardless of their order of appearance. This definition makes no reference to the exact sequence in which the field components cause the transition. Also, let $U_{ba}^n(\epsilon_{m_1},\ldots,\epsilon_{m_n})$ denote the amplitude of the field pathway $(\epsilon_{m_1},\ldots,\epsilon_{m_n})$, one term of which is shown in Eq. 6, and the remaining terms have the same form, but correspond to other permutations of the field components $\{\epsilon_{m_1},\ldots,\epsilon_{m_n}\}$. For example, the pathway $(\epsilon_{m_1},\epsilon_{m_2})$ has the amplitude $U_{ba}^2(\epsilon_{m_1},\epsilon_{m_2})$, given by

$$\begin{aligned} U_{ba}^2(\epsilon_{m_1},\epsilon_{m_2}) = \left(\frac{i}{\hbar}\right)^2 \Bigg[&\int_0^T\int_0^{t_2} \langle b|c_{m_2}\epsilon_{m_2}(t_2)\mu_I(t_2)c_{m_1}\epsilon_{m_1}(t_1)\mu_I(t_1)|a\rangle\, dt_1\, dt_2 \\ &+ \int_0^T\int_0^{t_2} \langle b|c_{m_1}\epsilon_{m_1}(t_2)\mu_I(t_2)c_{m_2}\epsilon_{m_2}(t_1)\mu_I(t_1)|a\rangle\, dt_1\, dt_2 \Bigg]. \end{aligned} \tag{7}$$

This amplitude contains two pathways from $|a\rangle$ to $|b\rangle$: one in which ϵ_1 is the initial interaction, and one in which ϵ_2 is the initial interaction. It will not always be necessary to specify the exact set of interactions, so for brevity, a generic nth order field pathway will be written as $\mathcal{M}_n$ instead of $(\epsilon_{m_1}, \ldots, \epsilon_{m_n})$, and the corresponding pathway amplitude will be denoted as $U^n_{ba}(\mathcal{M}_n)$. The complete transition element U_{ba}, which is the sum over all pathway amplitudes of all orders, may then be written

$$U_{ba} = \sum_{n=0}^{\infty} \sum_{\mathcal{M}_n} U^n_{ba}(\mathcal{M}_n). \tag{8}$$

The mechanism of the transition from $|a\rangle$ to $|b\rangle$ is specified by the collection of pathways with amplitudes of significant magnitude. The complex valued pathway amplitudes can interact constructively or destructively to produce the overall transition amplitude U_{ba}.

Each component of the control field may be encoded by a function $g_m(s)$, $g_m(0) = 1$, to create a set of control fields, parametrized by s, over the time interval $[0, T]$. The resulting encoded field is

$$\mathcal{E}(t, s) = \sum_{m=1}^{M} c_m \epsilon_m(t) g_m(s). \tag{9}$$

For any value of s, it is possible to use $\mathcal{E}(t, s)$ to drive the system dynamics over the interval $[0, T]$ and find the projection of the final wavefunction onto the target $|b\rangle$ as a function of s (i.e., $U_{ba}(s)$). In practice, the encoding in Eq. 9 would be achieved by using the pulse shaper to vary the pixels controlling phase and amplitude in such a way that the original (unencoded) control field satisfies $\mathcal{E}(t) \equiv \mathcal{E}(t, s = 0)$. Under encoding, the phase and amplitude pixels would be adjusted in a coordinated fashion over a sequence of experiments in which s is varied. The time evolution operator under the encoded control field is denoted $U_{ba}(s)$, and can be written as in [13],

$$U_{ba}(s) = \sum_{n=0}^{\infty} \sum_{\mathcal{M}_n} U^n_{ba}(\mathcal{M}_n) G^n_{ba}(s; \mathcal{M}_n), \tag{10}$$

where

$$G^n_{ba}(s; \mathcal{M}_n) = \prod_{i=1}^{n} g_{m_i}(s). \tag{11}$$

The power of HE lies in the form of Eq. 10 [11]. A suitable choice of the modulation functions ensures that each pathway amplitude $U^n_{ba}(\mathcal{M}_n)$ is associated with a unique function $G^n_{ba}(s; \mathcal{M}_n)$. The goal of determining mechanism is transformed from evaluation of the integrals in Eq. 5 to the problem of decomposing $U_{ba}(s)$ along a set of basis functions, $G^n_{ba}(s; \mathcal{M}_n)$. Mechanism is specified in terms of the significant pathway amplitudes $U^n_{ba}(\mathcal{M}_n)$, which are uncovered by evaluating $U_{ba}(s)$ over a

sufficient set of points $s_r \in \mathbb{R}^+$ and inverting the data stream. This problem, in both discrete and continuous state space settings, has been studied in works on computational HE [11–16]. However, with laboratory data, direct access to the Hamiltonian and the wavefunction is not available. Determining the decomposition of $U_{ba}(s)$ in terms of pathway amplitudes becomes a more difficult process because only $|U_{ba}(s)|^2$ is measurable (as well as other possible observables). Initial simulations show that laboratory based HE for mechanism extraction is possible [14], and the present paper addresses the fundamental issues raised by the use of observable information in HE.

3 Representation of the control field

While the representation of the control field is in principle arbitrary, the following representation has been chosen in order to develop working algorithms

$$\mathcal{E}(t) = A(t) \sum_{m=1}^{M} a_m \cos(\omega_m t + \phi_m). \tag{12}$$

This is a natural expression representative of the control fields generated by pulse-shapers in quantum control experiments. The nominal amplitudes $\{a_m\}$ and phases $\{\phi_m\}$ are assumed to be known, (e.g., from a closed-loop optimization procedure [1–10]). These same parameters will be modulated about their nominal values during the encoding process to produce three distinct schemes: amplitude modulation (A), phase modulation (P), and simultaneous modulation of the control amplitudes and phases (AP).

3.1 A-modulation

A-modulation works exclusively with the amplitude parameters $\{a_m\}$, to produce the modulated field form

$$\mathcal{E}(t, s) = A(t) \sum_{m=1}^{M} [a_m g_m(s)] \cos(\omega_m t + \phi_m). \tag{13}$$

Complete knowledge of mechanism in this representation corresponds to computing all significant amplitudes $U_{ba}^n(\mathcal{M}_n)$. Let $g_m(s) = \exp(\alpha_m s)$, with $\alpha_m \in \mathbb{R}$. Other forms of $g_m(s)$ for A-modulation could also be used. One advantage of using an exponential form is that products of the functions $g_m(s)$ are characterized by linear combinations of the parameters α_m. The resulting parametrized fields are

$$\mathcal{E}(t, s) = A(t) \sum_{m=1}^{M} a_m \exp(\alpha_m s) \cos(\omega_m t + \phi_m), \tag{14}$$

and the corresponding variation in $U_{ba}(s)$ is

$$U_{ba}(s) = \sum_{n=0}^{\infty} \sum_{\mathcal{M}_n} U_{ba}^{n}(\mathcal{M}_n) \exp\left[\left(\sum_{j=1}^{n} \alpha_{m_j}\right) s\right]. \tag{15}$$

The particular exponential coefficients $\{\alpha_m\}$ are specified by $\mathcal{M}_n$. We assume that the $\{\alpha_m\}$ are incommensurate, meaning that all of the sums $\sum_{j=1}^{n} \alpha_{m_j}$ are unique, at least up to a suitably high order n. Each product $G_{ba}^{n}(s; \mathcal{M}_n)$ of the modulating functions $g_m(s)$ has the form $\exp[(\sum_{j=1}^{n} \alpha_{m_j})s]$, making the set of all such functions, $\{G_{ba}^{n}(s; \mathcal{M}_n)\}$, linearly independent. If, for some large value of n the sum $\sum_{j=1}^{n} \alpha_{m_j}$ is not unique, then there will be multiple pathway amplitudes associated with a single modulating function. This situation is not expected to affect the mechanism analysis because these modulating functions, will generally correspond to high order pathway amplitudes which typically will be very small.

3.2 P-modulation

P-modulation utilizes just the phases $\{\phi_m\}$ to produce the encoded field

$$\mathcal{E}(t, s) = A(t) \sum_{m=1}^{M} a_m \cos(\omega_m t + [\phi_m + \gamma_m s]). \tag{16}$$

The control field can be written equivalently in exponential form

$$\mathcal{E}(t, s) = \sum_{m=1}^{M} \exp(i\gamma_m s) \exp(i\phi_m) a_m \epsilon_m^{+}(t) + \exp(-i\gamma_m s) \exp(-i\phi_m) a_m \epsilon_m^{-}(t), \tag{17}$$

where $i = \sqrt{-1}$. The basis functions of the field are $\epsilon_m^{\sigma}(t) = A(t) \exp(\sigma i \omega_m t)/2$, where $\sigma = +$ or $-$. The set of frequencies $\{\gamma_m\}$, which may be chosen at our discretion, is assumed to be incommensurate. Enumeration requires two indexes: m to denote the frequency component, and σ to denote the positive and negative frequencies. A typical pathway is $(\epsilon_{m_1}^{\sigma_1}, \ldots, \epsilon_{m_n}^{\sigma_n})$, with amplitude $U_{ba}^{n}(\epsilon_{m_1}^{\sigma_1}, \ldots, \epsilon_{m_n}^{\sigma_n})$, or $\mathcal{M}_n^{\Sigma}$ and $U_{ba}^{n}(\mathcal{M}_n^{\Sigma})$ in the compact notation, where Σ represents the n-tuple $(\sigma_1, \ldots, \sigma_n)$. Equation 10 becomes a Fourier series under P-modulation. This form can be conveniently inverted by Fourier transformation, as was done in previous work with computer simulations [11–13,15,16], and it is useful again with observation data [14].

In P-modulation, the modulating function $g_m^{+}(s) = \exp(i\gamma_m s)$, associated with ϵ_m^{+} is the inverse of the function $g_m^{-}(s) = \exp(-i\gamma_m s)$, associated with ϵ_m^{-}. For example, the pathway $(\epsilon_1^{+}, \epsilon_2^{-}, \epsilon_2^{+})$ has the modulation function $\exp(i(\gamma_1 - \gamma_2 + \gamma_2)s) = \exp(i\gamma_1 s)$, which is the same as the function corresponding to (ϵ_1^{+}). HE differentiates between pathways by introducing a unique modulation function for each pathway, but P-modulation may assign the same modulation function to certain sets of pathways, thus grouping them together into a pathway class. Such a pathway class is referred to

as a field composite pathway. For example, (ϵ_1^+) and $(\epsilon_1^+, \epsilon_2^-, \epsilon_2^+)$ belong to a single field composite pathway. The amplitude of the field composite pathway is the sum of the complex amplitudes of all the individual pathways within it. Since an interaction with ϵ_n^+ "cancels" an interaction with ϵ_n^-, each pathway class is determined by the "net" interaction. In the present example, the composite pathway $(\epsilon_1^+)^*$ contains the pathways (ϵ_1^+), $(\epsilon_1^+, \epsilon_2^+, \epsilon_2^-)$ and all pathways with a net interaction of ϵ_1^+, and its amplitude is denoted by $U_{ba}^1(\epsilon_1^+)^*$. Here, * indicates a class of composite pathways. Extracting mechanism in this representation corresponds to computing the amplitudes of all significant field composite pathways. The form of $U_{ba}(s)$ is

$$U_{ba}(s) = \sum_n \sum_{\mathcal{M}_n^{\Sigma *}} U_{ba}^n(\mathcal{M}_n^{\Sigma *}) \exp\left[i \left(\sum_{j=1}^n \sigma_j \gamma_{m_j} \right) s \right], \tag{18}$$

where each amplitude can be generated from a Fourier transform of $U_{ba}(s)$. For stability reasons, P-modulation is likely to be the most convenient scheme in terms of practical applications.

3.3 AP-modulation

The third possible modulation scheme combines A- and P-modulation into AP-modulation. In this scheme the encoded control field becomes

$$\mathcal{E}(t, s) = A(t) \sum_{m=1}^{M} \left[\exp(\alpha_m s) a_m \right] \cos\left(\omega_m t + \left[\phi_m + \gamma_m s \right] \right), \tag{19}$$

which may be written in exponential form

$$\begin{aligned} \mathcal{E}(t, s) = \sum_{m=1}^{m} \big\{ & \exp((\alpha_m + i\gamma_m)s) \exp(i\phi_m) a_m \epsilon_m^+(t) \\ & + \exp((\alpha_m - i\gamma_m)s) \exp(-i\phi_m) a_m \epsilon_m^-(t) \big\}. \end{aligned}$$

The variation in $U_{ba}(s)$ now becomes

$$U_{ba}(s) = \sum_{n=0}^{\infty} \sum_{\mathcal{M}_n^{\Sigma}} U_{ba}^n(\mathcal{M}_n^{\Sigma}) \exp\left[i \left(\sum_{j=1}^n \sigma_{m_j} \gamma_{m_j} \right) s + \left(\sum_{j=1}^n \alpha_{m_j} \right) s \right]. \tag{20}$$

Since AP-modulation resolves the control field along the same basis functions as P-modulation (despite the presence of the A-modulation basis functions), the individual pathways are identical. However, AP-modulation will also lift the "degeneracy" which created field composite pathways in P- modulation. Again consider the pair of pathways $(\epsilon_1^+, \epsilon_2^-, \epsilon_2^+)$ and (ϵ_1^+). In P-modulation they are both associated with the modulation function $\exp(i\gamma_1 s)$. However, in AP-modulation they have distinct

modulation functions $\exp((\alpha_1 + 2\alpha_2 + i\gamma_1)s)$ and $\exp((\alpha_1 + i\gamma_1)s)$, respectively. They are now distinguishable, and the amplitude of each individual pathway can be extracted. The P-modulation composite pathway amplitudes can be reconstructed from individual AP-modulation pathway amplitudes by summing up the amplitudes of all the pathways that contribute to a given field composite pathway.

To appreciate the connection between AP-modulation and A-modulation, consider the four AP-modulation pathways $(\epsilon_1^+, \epsilon_2^+)$, $(\epsilon_1^+, \epsilon_2^-)$, $(\epsilon_1^-, \epsilon_2^+)$, and $(\epsilon_1^-, \epsilon_2^-)$. If only A-modulation is applied, each pathway has the same modulation function, $\exp(i(\alpha_1 + \alpha_2)s)$. This happens because A-modulation encodes both ϵ_m^+ and ϵ_m^- with the same function of s, and hence cannot distinguish between them. All four AP-modulation pathways belong to the same A-modulation pathway (ϵ_1, ϵ_2). The amplitude of an A-modulation pathway can be explicitly reconstructed from the AP pathways

$$U_{ba}^n(\mathcal{M}_n) = \sum_{\Sigma} U_{ba}^n(\mathcal{M}_n^{\Sigma}) \tag{21}$$

where the sum is over all n-tuples $\Sigma = (\sigma_1, \ldots, \sigma_n)$. Therefore, a single A-modulation pathway corresponds to a pathway class in AP-modulation.

4 Assessing the solutions of the modulated equations

A-, P-, and AP-modulation create large systems of equations in the pathway amplitudes which must be solved to reveal mechanism. Any observable will be a quadratic form in the matrix elements of U. In this section we consider the effect of using the observable $|U_{ba}(s)|^2$ in order to solve for the pathway (or composite pathway) amplitudes. We show that using the observable form creates classes of equivalent, symmetry related solutions to these systems of equations. We give a definition for uniqueness and use a geometric illustration of HE to understand the symmetries which arise in the equations generated by observable based HE.

As background, consider the case of computer simulations. For all three forms of modulation we have the relation

$$U_{ba}(s) = \sum_{n=0}^{\infty} \sum_{\mathcal{M}_n^{\dagger}} U_{ba}^n(\mathcal{M}_n^{\dagger}) G_{ba}^n(s; \mathcal{M}_n^{\dagger}) \tag{22}$$

where the pathway $\mathcal{M}_n^{\dagger}$ may represent either $\mathcal{M}_n$ or $\mathcal{M}_n^{\Sigma}$, depending on the choice of modulation scheme. If there are r pathways with nonzero amplitudes, we may apply the following procedure: evaluate $U_{ba}(s)$ at r points $(s_1, \ldots, s_r)$, and write the resultant linear equation

$$\mathbf{A}x = y, \tag{23}$$

where $\mathbf{A}$ is an $r \times r$ matrix with $A_{rq} = G_{ba}^n(s_r; \mathcal{M}_{n,q}^{\dagger})$, x is the vector of pathway amplitudes $U_{ba}^n(\mathcal{M}_{n,q}^{\dagger})$, y is the vector of calculated data $U_{ba}(s_r)$, and the index q

has been added to $\mathcal{M}^{\dagger}_{n,q}$ in order to distinguish specific pathways. Since the functions $G^n_{ba}(s;\mathcal{M}^{\dagger}_{n,q})$ are linearly independent we can pick the values s_r to create a matrix $\mathbf{A}$ of full rank, and the linear system may then be solved. The independence is a result of careful construction, and does not follow merely from choosing linearly independent functions $g_m(s)$.[1] In the computational setting of HE, which allows access to the wavefunction, one just needs to solve the set of linear equations. The underlying physics guarantees the existence of a solution, and the linear independence of the modulating functions guarantees its uniqueness. The only constraining factor is numerical stability, and this was not an obstacle in previous numerical simulations [11,13], which were able to take advantage of the Fourier transform to perform inversion.

In the laboratory one needs to implement a decoding procedure which inverts the observable data $|U_{ba}(s)|^2$. When $|U_{ba}(s)|^2$ is used to extract mechanism, a quadratic system of equations

$$|U_{ba}(s)|^2 = \left| \sum_{n=0}^{\infty} \sum_{\mathcal{M}^{\dagger}_n} U^n_{ba}(\mathcal{M}^{\dagger}_n) G^n_{ba}(s;\mathcal{M}^{\dagger}_n) \right|^2, \tag{24}$$

needs to be solved. This raises questions about the uniqueness of the solutions. The concept of uniqueness needs to be understood in the context of certain symmetries, which arise due to the quadratic form of observables in quantum mechanics.

Four assumptions are made about the structure of the mechanism analysis.

Assumption 4.1 Existence: The equations are self consistent and a solution exists.

Assumption 4.2 A Maximum Contributing Order N Exists: All pathways with order higher than N have negligible amplitude.

Assumption 4.3 The Maximum Contributing Order is Known: N is known a priori.

Assumption 4.4 A Finite Representation of the Electric Field Exists: The electric field $\mathcal{E}(t)$ is exactly resolved into M component functions.

Assumption 4.1 is justified as the presence of an underlying physical mechanism gives rise to the HE equations. Consistency may only be approximately valid with real data, which will be contaminated by noise and measurement errors. Assumption 4.2 places a finite limit on the number of contributing pathways. For Assumption 4.3, a method to determine N is described in [14,16]. It is necessary to know that N is sufficiently large to produce a complete system of equations and uniquely determine the solution. If N is larger than necessary, then wasted searching for the extra null amplitudes can lead to instabilities, especially when dealing with noise contaminated data. Assumption 4.4 can always be arranged as the field is at our disposal in the laboratory.

[1] An example of a linearly independent set of functions that does not produce a linearly independent set of products is $\{1, 1+x, x^2\}$. The set of products produced by this set includes $(1)^2$, $(1)(1+x)$, $(1)(x^2)$ and $(1+x)^2 = (1+2x+x^2) = -1(1) + 2(1+x) + 1(x^2)$.

4.1 Impact of symmetry on the uniqueness of solutions

The control mechanism is specified by the collection of individual pathways of significant magnitude. HE distinguishes between different possible mechanisms by modulating individual pathway amplitudes. Each mechanistic pathway amplitude is complex valued and conveniently represented by a vector in the complex plane. The overall transition amplitude is a single vector, formed by aligning the individual pathway amplitudes head to tail in the complex plane. In the laboratory, only the absolute value squared of the overall amplitude is measurable. HE is able to determine the unknown pathway amplitudes $U^n_{ba}(\mathcal{M}^\dagger_n)$ by measuring the observable $|U_{ba}(s)|^2$, which is the left hand side of Eq. 24. If two different mechanisms lead to the same set of modulated observations, then HE cannot distinguish between them. The ability of HE to differentiate between distinct mechanisms is shown in Fig. 1. In the figure, the same unmodulated overall amplitude, U_{ba} in panel A and $\tilde{U}_{ba}$ in panel C, consists of three distinct amplitudes. A single AP-modulation scheme is capable of revealing that the underlying pathway amplitudes (i.e., the mechanisms) are different. There are some exceptions to this rule; certain symmetry related mechanisms are indistinguishable by laboratory based HE because the observable $|U_{ba}(s)|^2$ is invariant under these symmetry transformations. The geometric picture of pathway amplitudes as vectors provides graphical insight into these symmetries.

If two mechanisms are indistinguishable, then it is necessary that the following conditions are satisfied: (i) the lengths of the vectors are the same and (ii) the relative angles between the vectors representing the individual pathway amplitudes of each mechanism are the same. Geometrically, these conditions mean that the two mechanisms must be related by an *isometry* of the plane. Each vector in the first mechanism, $U^n_{ba}(\mathcal{M}^\dagger_n)$, must be related to its counterpart in the second mechanism, $\tilde{U}^n_{ba}(\mathcal{M}^\dagger_n)$, by that isometry. There are three isometries of the plane: translations, rotations and reflections. Translations are not relevant because only magnitude and direction are relevant when pathway amplitudes are identified as vectors.

Rotations correspond to a global change of phase, i.e. $\tilde{U}^n_{ba}(\mathcal{M}^\dagger_n) = \exp[i\theta]U^n_{ba}(\mathcal{M}^\dagger_n)$ for all $\mathcal{M}^\dagger_n$. Under the substitution $U^n_{ba}(\mathcal{M}^\dagger_n) \rightarrow \tilde{U}^n_{ba}(\mathcal{M}^\dagger_n)$ the observable is unchanged because

$$\begin{aligned}\left|\sum_{n=0}^{\infty}\sum_{\mathcal{M}^\dagger_n} U^n_{ba}(\mathcal{M}^\dagger_n)G^n_{ba}(s;\mathcal{M}^\dagger_n)\right|^2 &\rightarrow \left|\sum_{n=0}^{\infty}\sum_{\mathcal{M}^\dagger_n} \tilde{U}^n_{ba}(\mathcal{M}^\dagger_n)G^n_{ba}(s;\mathcal{M}^\dagger_n)\right|^2 \\ &= \left|\exp[i\theta]\sum_{n=0}^{\infty}\sum_{\mathcal{M}^\dagger_n} U^n_{ba}(\mathcal{M}^\dagger_n)G^n_{ba}(s;\mathcal{M}^\dagger_n)\right|^2 \\ &= \left|\sum_{n=0}^{\infty}\sum_{\mathcal{M}^\dagger_n} U^n_{ba}(\mathcal{M}^\dagger_n)G^n_{ba}(s;\mathcal{M}^\dagger_n)\right|^2 . \qquad (25)\end{aligned}$$

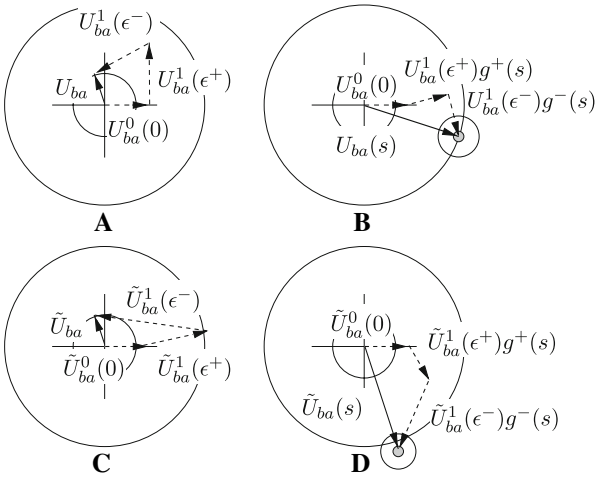

Fig. 1 Panel **A** shows the unmodulated overall amplitude U_{ba} (*solid arrow*) as the sum of three pathway amplitudes: $U^0_{ba}(0) + U^1_{ba}(\epsilon^+) + U^1_{ba}(\epsilon^-)$ (*dashed arrows*). These three pathway amplitudes $U^0_{ba}(0)$, $U^1_{ba}(\epsilon^+)$, and $U^1_{ba}(\epsilon^-)$ define the control mechanism. The circles in all of the panels have the same radii for comparative referencing. In Panel **B**, AP-modulation has scaled and rotated the pathway amplitudes. The amplitude $U^0_{ba}(0)$ is unchanged because it represents the contribution to U_{ba} of $\langle a|b\rangle$, which does not include interaction with the electric field. The measurable quantity in both **A** and **B** is the length of the solid arrow, or equivalently the radius of the inner and outer circles, respectively. A different mechanism is shown in panel **C**, consisting of the distinct contributing pathway amplitudes $\tilde{U}^0_{ba}(0)$, $\tilde{U}^1_{ba}(\epsilon^+)$, and $\tilde{U}^1_{ba}(\epsilon^-)$, and having the same unmodulated overall amplitude $\tilde{U}_{ba} = U_{ba}$, as for the mechanism in panel **A**. Under the same AP-modulation which transforms panel **A** to **B**, now **C** is transformed into the situation depicted in panel **D**. The two mechanisms underlying U_{ba} and $\tilde{U}_{ba}$ become distinguishable, because the same modulation applied to both cases results in different measurements (i.e., the length of the bold arrow in **D** is greater than the length of the bold arrow in **B**)

All rotations of a particular solution belong to the same solution class. This class can be categorized by a single arbitrarily chosen member; a convenient method is to select one pathway amplitude and give it a real, positive value. Figure 2 depicts two mechanisms related by rotation in the complex plane by an overall phase angle, and the figure demonstrates that the mechanisms are not distinguishable under AP-modulation. Physically, this isometry arises because a physical observable is invariant to an overall phase of the dynamically generated unitary transformation.

The remaining isometry is reflection, which is taken to be about the real axis because other reflections are a composition of this reflection and rotation. To find a transformation resulting in a reflection note that reflection about the real axis is the geometric equivalent of complex conjugation. Consider the case of P-modulation (the case for AP-modulation will be analogous). The modulating functions for the first order pathways (ϵ^+_m) and (ϵ^-_m) are $\exp[+i\gamma_m s]$ and $\exp[-i\gamma_m s]$, respectively. The modulating functions of these pathways are complex conjugates of each other, and generally the modulating functions of $\mathcal{M}^{\Sigma}_n$ and $\mathcal{M}^{\bar{\Sigma}}_n$ are also complex conjugates, where the superscript $\bar{\Sigma}$ is the conjugate of superscript Σ. Recall that in the compact notation, Σ represents the n-tuple, $(\sigma_1, \ldots, \sigma_n)$, and each σ_m corresponds to the sign of the complex part of the exponent in the modulating function (see for example Eq. 17 and

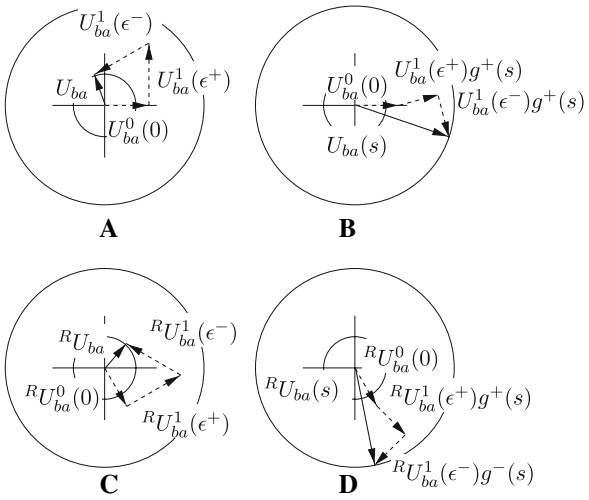

Fig. 2 For purposes of clarifying the notion of mechanistic equivalence under rotation by an overall phase, panels **A** and **B** are identical to the corresponding panels in Fig. 1. A new mechanism was created in panel **C** by a clockwise rotation (denoted by R) of the mechanism in panel **A**. The same AP-modulation used to transform **A** into **B** is used again to transform **C** into **D**. The resulting observable quantity, the length of $U_{ba}(s)$ in **B** and the length of ${}^RU_{ba}(s)$ in **D**, is the same in both cases. This behavior is a general property of mechanisms related by an overall rotation in the complex plane, and as a consequence the two unmodulated mechanisms depicted in **A** and **C** are not distinguishable

the subsequent paragraph). Thus, if Σ corresponds to $(+,-,-)$, then $\bar{\Sigma}$ is $(-,+,+)$. When two pathways are associated with conjugate modulating functions, we will refer to them as conjugate pathways. To see how reflection creates indistinguishable mechanisms under HE, consider the change of variables in which each pathway amplitude is replaced by the complex conjugate of the amplitude for its conjugate pathway

$$U^n_{ba}(\mathcal{M}^{\Sigma}_n) \rightarrow \bar{U}^n_{ba}(\mathcal{M}^{\bar{\Sigma}}_n). \tag{26}$$

To see why Eq. 24 is invariant under this transformation, expand the right hand side of the equation. Each term in the resulting sum will be the product of a coefficient (a pair of pathway amplitudes) and a function of s (a pair of modulating functions). The coefficient, $U^n_{ba}(\mathcal{M}^{\Sigma}_n)\bar{U}^{n'}_{ba}(\mathcal{M}^{\Sigma'}_{n'})$ and its replacement under Eq. 26, $\bar{U}^n_{ba}(\mathcal{M}^{\bar{\Sigma}}_n)U^{n'}_{ba}(\mathcal{M}^{\bar{\Sigma}'}_{n'})$, both correspond to the same function of s, $\exp[(\mathcal{A}+i\Gamma)s]$ where $\Gamma = \sum_{j=1}^{n}\sigma_j\gamma_{m_j} - \sum_{j=1}^{n'}\sigma'_j\gamma_{m'_j}$, and $\mathcal{A} = \sum_{j=1}^{n}\alpha_{m_j} + \alpha_{m'_j}$ ($\mathcal{A} = 0$ for P-modulation). That is

$$G(s;\mathcal{M}^{\Sigma}_n)\overline{G(s;\mathcal{M}^{\Sigma'}_{n'})} = \overline{G(s;\mathcal{M}^{\bar{\Sigma}}_n)}G(s;\mathcal{M}^{\bar{\Sigma}'}_{n'}). \tag{27}$$

It is also true that if any coefficient appears on the right hand side of Eq. 24, then so does its replacement (some coefficients are unchanged by Eq. 26, so they replace themselves). This means that these pairs of coefficients exchange roles when the substitution from Eq. 26 is applied, and the result is that Eq. 24 is left unchanged.

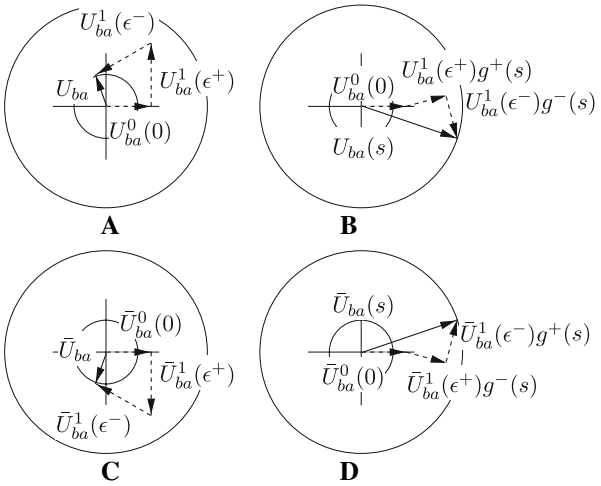

Fig. 3 For comparison, panels **A** and **B** are identical to the corresponding panels in Fig. 1. A symmetry related mechanism is shown in panel **C**, which is related to the mechanism in panel **A** by reflection about the real axis. This operation is equivalent to complex conjugation of the pathway amplitudes. AP-modulation is used to transform **A** into **B**. The conjugated form of the same modulation is then applied to **C** to produce **D**. Note that, due to AP-modulation, the conjugate pathways (ϵ^+) and (ϵ^-) exchanged amplitudes under reflection. The practical effect of this is that $\bar{U}^1_{ba}(\epsilon^+)$ is modulated by $g^-(s)$ and $\bar{U}^1_{ba}(\epsilon^-)$ is modulated by $g^+(s)$. The resulting observable quantity, the length of $U_{ba}(s)$ in **B** and the length of $\bar{U}_{ba}(s)$ in **D**, is the same in both cases. This is a general property of mechanisms related by reflection symmetry, and as a consequence the two unmodulated mechanisms depicted in **A** and **C** are physically indistinguishable

Geometrically, this substitution reflects each pathway amplitude about the real axis. However, each amplitude has not only been reflected, but it has also been reassigned from one pathway to that pathway's conjugate. In effect this is an exchange of labels between the pairs of conjugate pathway amplitudes. The same argument applies to A-modulation, however, since the modulating functions are real valued, each pathway is its own conjugate pathway and no relabeling occurs, just reflection. We will refer to the transformation in Eq. 26 as reflection symmetry, but it is to be understood that it also includes the exchange of pathway labels between conjugate pathways for P- or AP-modulation. The reflection symmetry under AP-modulation is depicted in Fig. 3. The only visible change is that each pathway amplitude seems to have rotated, between panels C and D, in the direction counter to that between panels A and B. The modulation applied is the same in both cases, but the pairs of conjugate pathway amplitudes have exchanged roles. The consequence of this is that if a pathway amplitude had been modulated by $G^n_{ba}(s;\mathcal{M}^{\Sigma}_n) = \exp[(\mathcal{A}+i\Gamma)s]$, then after applying the substitution from Eq. 26 it will be modulated by $G^n_{ba}(s;\mathcal{M}^{\bar{\Sigma}}_n) = \exp[(\mathcal{A}-i\Gamma)s]$. The magnitude of dilation and rotation of the amplitude is the same in both cases, but the direction that the pathway amplitude rotates due to the modulation is reversed. Sometimes, as will be shown later, physical insight can be used to lift the exchange of labels caused by reflection symmetry.

In summary, for any mechanism, a family of equivalent rotated and conjugated mechanisms can be generated. The remainder of this work considers two mechanisms to be unique, if they are not related by any linear combination of these symmetries.

4.2 Extracting pathways from observable data

If there are N pathways with significant amplitudes, there will be N distinct functions $G^n_{ba}(s;\mathcal{M}^\dagger_n)$ in Eq. 22. The right hand side of Eq. 24 will produce all pairwise products of the modulating functions: $G^n_{ba}(s;\mathcal{M}^\dagger_n)\bar{G}^m_{ba}(s;\mathcal{M}^\ddagger_m)$. While the set of functions $\{G^n_{ba}(s;\mathcal{M}^\dagger_n)\}$ is linearly independent, the set of *all* products of these functions may not share this property. This outcome can happen as not all of these products may be unique, i.e., $G^n_{ba}(s;\mathcal{M}^\dagger_n)\bar{G}^m_{ba}(s;\mathcal{M}^\ddagger_m) = G^{n'}_{ba}(s;\mathcal{M}^{\dagger'}_{n'})\bar{G}^{m'}_{ba}(s;\mathcal{M}^{\ddagger'}_{m'})$ does not necessarily imply that $n, m, \dagger$, and $\ddagger$ are equal to their primed counterparts. The number of distinct products obtained in Eq. 24 depends on the modulation scheme and the particular pathways which are present. The set of all *distinct* s-function products is linearly independent, at least for the exponential modulation functions considered here. As noted at the beginning of Sect. 4, not all families of linearly independent functions share this property.

Each distinct product of s functions, $G^n_{ba}(s;\mathcal{M}^\dagger_n)\bar{G}^m_{ba}(s;\mathcal{M}^\ddagger_m)$ in the expansion of $|U_{ba}(s)|^2$ corresponds to at least one, but possibly several, pathway products of the form $U^{n'}_{ba}(\mathcal{M}^{\dagger'}_{n'})\bar{U}^{m'}_{ba}(\mathcal{M}^{\ddagger'}_{m'})$. Two steps are needed to extract the individual pathway amplitudes $U^n_{ba}(\mathcal{M}^\dagger_n)$. The first step is to write $|U_{ba}(s)|^2$ as a linear combination of the distinct s-function products (d$s$fp)

$$\begin{aligned}|U_{ba}(s)|^2 &= \sum_{\mathrm{d}s\mathrm{fp}}\left(\sum_{\mathrm{prime}} U^{n'}_{ba}(\mathcal{M}^{\dagger'}_{n'})\bar{U}^{m'}_{ba}(\mathcal{M}^{\ddagger'}_{m'})\right) G^n_{ba}(s;\mathcal{M}^\dagger_n)\bar{G}^m_{ba}(s;\mathcal{M}^\ddagger_m)\\ &= \sum_{\mathrm{d}s\mathrm{fp}} k_{\mathrm{d}s\mathrm{fp}} G^n_{ba}(s;\mathcal{M}^\dagger_n)\bar{G}^m_{ba}(s;\mathcal{M}^\ddagger_m),\end{aligned} \tag{28}$$

where the inner sum is over all primed variables that correspond to pathway amplitude products which are modulated by $G^n_{ba}(s;\mathcal{M}^\dagger_n)\bar{G}^m_{ba}(s;\mathcal{M}^\ddagger_m)$. This is a *linear* equation, and will yield a *unique* solution for the coefficients $k_{\mathrm{d}s\mathrm{fp}}$, as all of the pairwise s-function products are mutually independent. However, each coefficient $k_{\mathrm{d}s\mathrm{fp}}$ may correspond to more than one pathway product. Determining the coefficients $k_{\mathrm{d}s\mathrm{fp}}$ by utilizing the linear independence of the products $G^n_{ba}(s;\mathcal{M}^\dagger_n)G^m_{ba}(s;\mathcal{M}^\ddagger_m)$, results in a set of quadratic equations in the pathway amplitudes

$$k_{\mathrm{d}s\mathrm{fp}} = \sum_{\mathrm{prime}} U^{n'}_{ba}(\mathcal{M}^{\dagger'}_{n'})\bar{U}^{m'}_{ba}(\mathcal{M}^{\ddagger'}_{m'}). \tag{29}$$

Each pathway amplitude may be written as the sum of its real and imaginary parts, $U^n_{ba}(\mathcal{M}^\dagger_n) = x_\eta + iy_\eta$, where $\eta = \mathcal{M}^\dagger_n$ is used to unburden the notation. This makes

Eq. 29 a collection of homogeneous quadratic equations in the real variables $\{x_\eta, y_\eta\}$. The remaining step is to solve this system of equations to obtain the unknown pathway amplitudes.

The analysis in Sect. 4.1 implies that there are two fundamental symmetries arising within quantum mechanics that prevent the unique determination of $\{x_\eta, y_\eta\}$. The issue of concern is the possible existence of a second solution $\{x_{\eta'}, y_{\eta'}\}$ not related to the $\{x_\eta, y_\eta\}$ by any symmetry. The fact (shown in Sect. 5) that HE will generate a heavily overdetermined system of equations to solve for the mechanistic pathway amplitudes makes the existence of multiple solutions, unrelated by a symmetry operation, unlikely.

5 Counting the numbers of variables and equations

Generally, more equations than variables are needed to uniquely determine the solution to a nonlinear system of equations [17], but it is not immediately clear that the modulation schemes will produce overdetermined systems. This section demonstrates that each modulation scheme can produce more than enough independent equations to carry out HE. The formulas are derived in the Appendix.

Assumption 4.2 in Sect. 4 states that only pathway amplitudes up to some order N contribute. Under this assumption, all of the pathway amplitude products in Eq. 29 are of an order lying in the range 0 to $2N$. It is convenient to consider using equations up to order $B < 2N$, and finding the smallest value of B such that HE generates a sufficient number of equations. This procedure is employed because the assumption of a finite cutoff order N is an approximation, and using $B < 2N$ limits potential contamination from higher order terms. B will be referred to as the utilized order, and N as the underlying order. B will always lie between N and $2N$.

The technique for counting the number of equations and variables is similar for all three modulation procedures, A, P, and AP. The details vary in each case, as sketched in the following subsections. The complex value of each pathway amplitude needs to be taken into account, and a full treatment can be found in the Appendix.

5.1 A-modulation

The number of variables (i.e., twice the number of identifiable pathway amplitudes) arising from A-modulation depends on M, the number of field components and N, the underlying order. The factor of two in the following formula accounts for the separate real and imaginary components of each pathway amplitude. The total number of variables is

$$v = 2\sum_{n=0}^{N} \binom{M-1+n}{M-1}. \tag{30}$$

The number of equations e produced by A-modulation only depends on M and B

$$e = \sum_{b=0}^{B} \binom{M-1+b}{M-1}. \tag{31}$$

Consider the two cases, $B = N$ and $B = 2N$. In the former case when the underlying and utilized orders are equal, the number of variables is twice the number of equations. This means that B must be greater than N, regardless of the value of M, or the system of equations will be underdetermined. However, when $B = 2N$, the system is overdetermined for all M except $M = 1$. If $M = 1$, and $B = 2N$, then the number of variables is always one more than the number of equations, so the system is underdetermined. This result means that at least two field components are necessary to produce an overdetermined system. In practice M may be much larger than 1 (possibly even $\sim 10^2$ or more). A significant property of Eqs. 30 and 31 occurs in the limit of large M. If $M > N^2 + N + 1$, then it suffices to use $B = N + 1$ in order to obtain more equations than variables.

It is possible to verify these formulas in low order cases by exhaustively enumerating the equations and variables. For an explicit example let $M = 2$, with the A-modulation functions $\exp[\alpha_m s]$ and $m \in \{1, 2\}$. If $N = 2$, then the twelve variables predicted by Eq. 30 correspond to the real and imaginary parts of the pathway amplitudes with modulating exponents $0, \alpha_1, \alpha_2, 2\alpha_1, \alpha_1 + \alpha_2$, and $2\alpha_2$. If $B = 3$, then Eq. 31 predicts ten equations. Upon expanding Eq. 24, 10 unique exponents arise: $0, \alpha_1, \alpha_2, 2\alpha_1, \alpha_1 + \alpha_2, 2\alpha_2, 3\alpha_1, 2\alpha_1 + \alpha_2, \alpha_1 + 2\alpha_2$, and $3\alpha_2$. This approach was used to verify the expressions above for all cases $(M, N, B) \in \{1 \ldots 5\} \times \{1 \ldots 5\} \times \{N \ldots 2N\}$.

5.2 AP-modulation

Counting the variables produced by AP-modulation is very similar to that of A-modulation. Consider, for example, the (ϵ_1, ϵ_2) pathway produced by A-modulation, which splits into four pathways under AP-modulation, $(\epsilon_1^+, \epsilon_2^+)$, $(\epsilon_1^+, \epsilon_2^-)$, $(\epsilon_1^-, \epsilon_2^+)$, and $(\epsilon_1^-, \epsilon_2^-)$. Splitting ϵ_m into ϵ_m^+ and ϵ_m^- effectively doubles the number of field components. The total number of variables is

$$v = 2 \sum_{n=0}^{N} \binom{2M-1+n}{2M-1}, \tag{32}$$

which is Eq. 30 with M replaced by $2M$. The same argument holds true for the number of equations

$$e = \sum_{b=0}^{B} \binom{2M-1+b}{2M-1}. \tag{33}$$

The results of the extremal cases $B = N$ and $B = 2N$ are the same as before, except now $B = 2N$ is sufficient even in the case $M = 1$. Also, $B = N+1$ will create an over-

determined system if $M > (N^2+N+1)/2$. As with the A-modulation case, the formulas in this section were independently verified through computational enumeration of the variables and equations in all cases $(M, N, B) \in \{1 \ldots 5\} \times \{1 \ldots 5\} \times \{N \ldots 2N\}$.

5.3 P-modulation

While A- and AP-modulation yielded nearly identical formulas for the numbers of variables and equations, P-modulation presents a distinct analysis. The same field component doubling as in AP-modulation occurs, therefore there are $2M$ components. P-modulation defines field composite pathways in terms of "net" interactions with field components. Therefore, each field composite pathway may contain either ϵ_m^+ or ϵ_m^-, but not both. The final expression for the number of variables is

$$v = 2\left(1 + 2M + \sum_{n=2}^{N} \sum_{k=1}^{\min(M,n)} 2^k \binom{M}{k} \binom{n-1}{k-1}\right), \tag{34}$$

where $\min(M, n)$ ensures that ϵ_j^+ and ϵ_j^- are not simultaneously selected. The number of equations is

$$e = 1 + 2M + \sum_{b=2}^{B} \sum_{k=1}^{\min(M,b)} 2^k \binom{M}{k} \binom{b-1}{k-1}. \tag{35}$$

As with A-modulation, $B = N$ is not sufficient, because it implies that the number of variables is twice the number of equations. Again, $B = 2N$ is sufficient for all values of M, as is $B = N + 1$ in the limit of large M. The formulas for the number of variables and equations were again verified computationally for the cases $(M, N, B) \in \{1 \ldots 5\} \times \{1 \ldots 5\} \times \{N \ldots 2N\}$.

The analysis above completes the case for establishing the existence of overdetermined sets of equations in observable based HE. We shall now look at the general solution of a model system, and then consider a more specific example.

6 Illustration

6.1 General solution to a model system

This section presents a simple example of HE, including its analytic solution. The case under consideration is $(M, N, B) = (2, 1, 2)$ using AP-modulation. The expressions in Sect. 5.2 show that the system has $2 \times 5 = 10$ variables and 15 equations. The variables are the real and imaginary parts of the pathway amplitudes $\{U_{ba}^0(0), U_{ba}^1(\epsilon_1^+), U_{ba}^1(\epsilon_1^-), U_{ba}^1(\epsilon_2^+), U_{ba}^1(\epsilon_2^-)\}$; here (0) indicates the non-interacting, and therefore unmodulated, zeroth order pathway, $\langle a|b\rangle$. Equation 24 becomes

$$
\begin{aligned}
|U_{ba}(s)|^2 = \Big| & U^0_{ba}(0)\exp[0s] + U^1_{ba}(\epsilon_1^+)\exp[(\alpha_1 + i\beta_1)s] \\
& + U^1_{ba}(\epsilon_1^-)\exp[(\alpha_1 - i\beta_1)s] + U^1_{ba}(\epsilon_2^+)\exp[(\alpha_2 + i\beta_2)s] \\
& + U^1_{ba}(\epsilon_2^-)\exp[(\alpha_2 - i\beta_2)s]\Big|^2 . \qquad (36)
\end{aligned}
$$

After expanding the right hand side of Eq. 36, the result is a specific instance of Eq. 28, which is a linear system, $Au = v$, in the pathway products. Here A, u, and v have the following components

$$u_q = \sum_{(j,k)\sim(\mathcal{A}+i\Gamma)_q} U^1_{ba}(\epsilon^{\sigma_j}_{m_j})\bar{U}^1_{ba}(\epsilon^{\sigma_k}_{m_k}), \qquad (37)$$

$$A_{rq} = \exp[((\alpha_j^{\sigma_j} + \alpha_k^{\sigma_k}) + i(\gamma_j^{\sigma_j} - \gamma_k^{\sigma_k}))s_r] = \exp[(\mathcal{A} + i\Gamma)_q s_r], \qquad (38)$$

$$v_r = |U_{ba}(s_r)|^2. \qquad (39)$$

Each pair (j, k) corresponds to an exponent $(\mathcal{A} + i\Gamma)_q$, and the sum in Eq. 37 is over all (j, k) that produce $(\mathcal{A} + i\Gamma)_q$.

Fully expanded, each modulated observation $v_r = |U_{ba}(s_r)|^2$ is

$$
\begin{pmatrix}
\exp[0] \\
\exp[2\alpha_1 s_r] \\
\exp[2\alpha_2 s_r] \\
\exp[(\alpha_1 - i\beta_1)s_r] \\
\exp[(\alpha_1 + i\beta_1)s_r] \\
\exp[(\alpha_2 - i\beta_2)s_r] \\
\exp[(\alpha_2 + i\beta_2)s_r] \\
\exp[(2\alpha_1 + 2i\beta_1)s_r] \\
\exp[(2\alpha_1 - 2i\beta_1)s_r] \\
\exp[(2\alpha_2 + 2i\beta_2)s_r] \\
\exp[(2\alpha_2 - 2i\beta_2)s_r] \\
\exp[((\alpha_1 + \alpha_2) + i(\beta_1 + \beta_2))s_r] \\
\exp[((\alpha_1 + \alpha_2) - i(\beta_1 + \beta_2))s_r] \\
\exp[((\alpha_1 + \alpha_2) + i(\beta_1 - \beta_2))s_r] \\
\exp[((\alpha_1 + \alpha_2) - i(\beta_1 - \beta_2))s_r]
\end{pmatrix}^T
\times
\begin{pmatrix}
U^0_{ba}(0)\bar{U}^0_{ba}(0) \\
U^1_{ba}(\epsilon_1^+)\bar{U}^1_{ba}(\epsilon_1^+) + U^1_{ba}(\epsilon_1^-)\bar{U}^1_{ba}(\epsilon_1^-) \\
U^1_{ba}(\epsilon_2^+)\bar{U}^1_{ba}(\epsilon_2^+) + U^1_{ba}(\epsilon_2^-)\bar{U}^1_{ba}(\epsilon_2^-) \\
U^0_{ba}(0)\bar{U}^1_{ba}(\epsilon_1^+) + U^1_{ba}(\epsilon_1^-)\bar{U}^0_{ba}(0) \\
U^1_{ba}(\epsilon_1^+)\bar{U}^0_{ba}(0) + U^0_{ba}(0)\bar{U}^1_{ba}(\epsilon_1^-) \\
U^0_{ba}(0)\bar{U}^1_{ba}(\epsilon_2^+) + U^1_{ba}(\epsilon_2^-)\bar{U}^0_{ba}(0) \\
U^1_{ba}(\epsilon_2^+)\bar{U}^0_{ba}(0) + U^0_{ba}(0)\bar{U}^1_{ba}(\epsilon_2^-) \\
U^1_{ba}(\epsilon_1^+)\bar{U}^1_{ba}(\epsilon_1^-) \\
U^1_{ba}(\epsilon_1^-)\bar{U}^1_{ba}(\epsilon_1^+) \\
U^1_{ba}(\epsilon_2^+)\bar{U}^1_{ba}(\epsilon_2^-) \\
U^1_{ba}(\epsilon_2^-)\bar{U}^1_{ba}(\epsilon_2^+) \\
U^1_{ba}(\epsilon_1^+)\bar{U}^1_{ba}(\epsilon_2^-) + U^1_{ba}(\epsilon_2^+)\bar{U}^1_{ba}(\epsilon_1^-) \\
U^1_{ba}(\epsilon_2^-)\bar{U}^1_{ba}(\epsilon_1^+) + U^1_{ba}(\epsilon_1^-)\bar{U}^1_{ba}(\epsilon_2^+) \\
U^1_{ba}(\epsilon_1^+)\bar{U}^1_{ba}(\epsilon_2^+) + U^1_{ba}(\epsilon_2^-)\bar{U}^1_{ba}(\epsilon_1^-) \\
U^1_{ba}(\epsilon_2^+)\bar{U}^1_{ba}(\epsilon_1^+) + U^1_{ba}(\epsilon_1^-)\bar{U}^1_{ba}(\epsilon_2^-)
\end{pmatrix}
\qquad (40)
$$

After choosing 15 values $s_0 = 0$ through s_{14}, evaluating A directly and v by measuring $|U_{ba}(s_r)|^2$, the resulting linear system may be solved to find the values u_q. Next, let $U^n_{ba}(\epsilon^{\sigma_j}_{m_j}) = x^{\sigma_j}_{m_j} + iy^{\sigma j}_{m_j}$ and the result is the following system of quadratic equations

$$u = \begin{pmatrix} u_0 \\ u_1 \\ u_2 \\ u_3 \\ u_4 \\ u_5 \\ u_6 \\ u_7 \\ u_8 \\ u_9 \\ u_{10} \\ u_{11} \\ u_{12} \\ u_{13} \\ u_{14} \end{pmatrix} = \begin{pmatrix} x_0^2 + y_0^2 \\ x_0(x_1^+ + x_1^-) + y_0(y_1^+ + y_1^-) \\ x_0(x_2^+ + x_2^-) + y_0(y_2^+ + y_2^-) \\ x_0(-y_1^+ + y_1^-) + y_0(x_1^+ - x_1^-) \\ x_0(-y_2^+ + y_2^-) + y_0(x_2^+ - x_2^-) \\ (x_1^+)^2 + (y_1^+)^2 + (x_1^-)^2 + (y_1^-)^2 \\ (x_2^+)^2 + (y_2^+)^2 + (x_2^-)^2 + (y_2^-)^2 \\ x_1^+ x_1^- + y_1^+ y_1^- \\ x_2^+ x_2^- + y_2^+ y_2^- \\ -x_1^+ y_1^- + x_1^- y_1^+ \\ -x_2^+ y_2^- + x_2^- y_2^+ \\ x_1^+ x_2^+ + y_1^+ y_2^+ + x_1^- x_2^- + y_1^- y_2^- \\ -x_1^+ y_2^+ + y_1^+ x_2^+ + x_1^- y_2^- - y_1^- x_2^- \\ x_1^+ x_2^- + y_1^+ y_2^- + x_1^- x_2^+ + y_1^- y_2^+ \\ -x_1^+ y_2^- + y_1^+ x_2^- + x_1^- y_2^+ - y_1^- x_2^+ \end{pmatrix}. \tag{41}$$

This quadratic system of equations has an analytic solution, which is unique up to the symmetries discussed in Sect. 4.1. To solve the system, we may first fix the overall phase by setting $y_0 = 0$ and $x_0 = +\sqrt{u_0}$. From this foundation, the equations for u_1 through u_{10} can be used to determine the following reflection related solutions in terms of the parameters $k_j^\pm$

$$\begin{aligned} k_1^\pm &= (u_5 \pm \sqrt{u_5^2 - 4(u_7^2 + u_9^2)})/2 \\ k_2^\pm &= (u_6 \pm \sqrt{u_6^2 - 4(u_8^2 + u_{10}^2)})/2 \end{aligned} \tag{42}$$

$$\begin{aligned} y_0 &= 0 \\ x_0 &= +\sqrt{u_0} \\ x_1^- &= \frac{k_1^\pm}{u_0} \frac{(u_1u_7 - u_3u_9 - u_1k_1^\pm)x_0 + (u_1u_9 + u_3u_7 + u_3k_1^\pm)y_0}{u_7^2 + u_9^2 - (k_1^\pm)^2} \\ y_1^- &= -\frac{k_1^\pm}{u_0} \frac{(u_3u_7 + u_1u_9 + u_3k_1^\pm)x_0 + (u_3u_9 - u_1u_7 + u_1k_1^\pm)y_0}{u_7^2 + u_9^2 - (k_1^\pm)^2} \\ x_2^- &= \frac{k_2^\pm}{u_0} \frac{(u_2u_8 - u_4u_{10} - u_2k_2^\pm)x_0 + (u_2u_{10} + u_4u_8 + u_4k_2^\pm)y_0}{u_8^2 + u_{10}^2 - (k_2^\pm)^2} \\ y_2^- &= -\frac{k_2^\pm}{u_0} \frac{(u_2u_{10} + u_4u_8 + u_4k_2^\pm)x_0 + (u_4u_{10} - u_2u_8 + u_2k_2^\pm)y_0}{u_8^2 + u_{10}^2 - (k_2^\pm)^2} \\ x_1^+ &= (u_7x_1^- - u_9y_1^-)/k_1^\pm \\ y_1^+ &= (u_9x_1^- + u_7y_1^-)/k_1^\pm \\ x_2^+ &= (u_8x_2^- - u_{10}y_2^-)/k_2^\pm \\ y_2^+ &= (u_{10}x_2^- + u_8y_2^-)/k_2^\pm. \end{aligned} \tag{43}$$

This was derived assuming that all of the pathways present are non-zero. The reflection symmetry will be fixed by selecting k_j^+ or k_j^- for $j = 1, 2$, and the equations which have not yet been used (those for u_{11} through u_{14}) will determine the sign choice for $k_j^\pm$ in Sect. 6.2.

Reflection symmetry is naturally present here. The mechanism cannot be conclusively defined as the set of five pathway amplitudes; $\{U_{ba}^0(0), U_{ba}^1(\epsilon_1^+), U_{ba}^1(\epsilon_1^-), U_{ba}^1(\epsilon_2^+), U_{ba}^1(\epsilon_2^-)\}$, as well as $\{\bar{U}_{ba}^0(0), \bar{U}_{ba}^1(\epsilon_1^+), \bar{U}_{ba}^1(\epsilon_1^-), \bar{U}_{ba}^1(\epsilon_2^+), \bar{U}_{ba}^1(\epsilon_2^-)\}$ each form an acceptable mechanism. In a specific instance of these equations, with values drawn from a laboratory experiment, one would find two complex values corresponding to $U_{ba}^1(\epsilon_j^+)$ and $U_{ba}^1(\epsilon_j^-)$. However, it would not be possible to decide which value should be assigned to a particular pathway amplitude. To resolve this issue consider the set, $\{U_{ba}^0(0), U_{ba}^1(\epsilon_1^+) + U_{ba}^1(\epsilon_1^-), U_{ba}^1(\epsilon_2^+) + U_{ba}^1(\epsilon_2^-)\}$ defining a reduced mechanism. If this set is used to define the reduced mechanism, then the ambiguity is removed regarding the reflection symmetry exchange of labels, i.e., it is no longer possible to mistakenly identify $U_{ba}^1(\epsilon_i^+)$ as $U_{ba}^1(\epsilon_i^-)$. To obtain $U_{ba}^1(\epsilon_1^+) + U_{ba}^1(\epsilon_1^-)$, one may solve for $U_{ba}^1(\epsilon_1^+)$ and $U_{ba}^1(\epsilon_1^-)$ separately and then sum the two values. The simple reflection symmetry will persist, but the labeling of pathway amplitude classes will be certain.

The solution derived in this section is readily extended to any higher value of M. It is significantly more difficult to extend it to higher order pathways (larger values of N) and obtain analytic solutions. Larger values of M and N greatly increase the number of terms involved in Eqs. 40 and 41, but do not alter their basic structure.

6.2 Symmetries arising in the solution

This section contains a numerical solution to the example in the previous section in order to illustrate the fundamental symmetries discussed previously in Sect. 4.1. The true mechanism in this example was produced by randomly selecting values for each amplitude $U_{ba}^n(\epsilon_{m_j}^{\sigma_j})$, which are listed in the final column of Table 1. The true solution was then inserted into the right hand side of Eq. 40 and used to produce observable values $|U_{ba}(s_r)|^2$. Once the observable data was produced, the mechanism extraction process was performed in the same way it would be with laboratory data.

Table 1 Pathway amplitude values for the numerical solution and the true solution

Pathway amplitude	Numerical solution	Numerical solution with rotation	True solution
$U_{ba}^0(0)$	0.2356+0.0000i	$-0.2039 + 0.1180i$	$-0.2040-0.1180i$
$U_{ba}^1(\epsilon_1^+)$	$-0.2722-0.9543i$	$-0.4115 + 0.1136i$	$-0.4115-0.1136i$
$U_{ba}^1(\epsilon_1^-)$	0.4131+0.1077i	$0.7134 + 0.6900i$	$0.7134-0.6900i$
$U_{ba}^1(\epsilon_2^+)$	0.2620+0.4492i	$0.2440 - 0.0673i$	0.2440+0.0672i
$U_{ba}^1(\epsilon_2^-)$	$-0.2449-0.0639i$	$-0.4517 - 0.2577i$	$-0.4517+0.2577i$

In the third column, each pathway amplitude in the numerical solution has been rotated by an overall phase which was chosen to align the pathway amplitude $U_{ba}^0(0)$ with the true solution

The values of u_q are found by solving the linear system in Eqs. 37–39. The condition number of the matrix $A_{r,q}$ depends on the values α_j, and the range over which s is allowed to vary. In this example $\alpha_1 = 1/10, \alpha_2 = \sqrt{2}/10, \beta_1 = 1, \beta_2 = \sqrt{2}$, and $s \in [0, 2\pi]$. These values ensure that the exponents which result from modulation and squaring are incommensurate up to an acceptably high order of pathway products. Next, the complex pathway products, $(x_j^{\sigma_j} + iy_j^{\sigma_j})\overline{(x_k^{\sigma_k} + iy_k^{\sigma_k})}$, were expanded, and the real and imaginary parts were identified to produce the system of quadratic equations, Eq. 41. With the values u_q in hand, the solution in Eq. 43 was evaluated. In this example, the following parameters were used to determine the solution: $y_0 = 0, x_0 = \sqrt{u_0}, k_1^+$, and k_2^+. All of the equations in Eq. 41 were used to verify the solution. A very small, but non-zero numerical error was present in each equation. The numerically derived pathway values are printed in the second column of Table 1.

The pathways in the second and fourth columns of Table 1, respectively, corresponding to the numerically derived and true solutions, are difficult to compare because an overall phase difference is present. Since rotations generate equivalent solutions to the quadratic system, we may choose one pathway as a reference, (0) in this case, and rotate all of the derived pathways by an angle so that the derived pathway amplitude $U_{ba}^0(0)$ and the true pathway amplitude $U_{ba}^0(0)$ coincide. The result of rotating all of the derived pathways by -2.617 radians is listed in column three of Table 1, and it clearly shows agreement with the true solution. Another convenient and equivalent measure is to specify the magnitudes and relative angles between pathways.

Table 1 reveals that the parameter choice (k_1^+, k_2^+) yields the true solution, and not its reflected counterpart. If the parameters (k_1^-, k_2^-) are used instead, then the derived mechanism is the reflected version of the true solution. If either pair of "mixed sign" parameters (k_1^+, k_2^-) or (k_1^-, k_2^+) are used, however, the extra equations (those for u_{11} through u_{14}) are not satisfied, eliminating these possibilities. It is important to note that both "same sign" choices are consistent with the true mechanism and lead to distinct symmetry related solutions which completely satisfy the system of Eqs. 41.

One way to lift the exchange component of the reflection symmetry is to sum the pairs of conjugate pathways which cause the ambiguity, as suggested at the end of Sect. 6.1. Magnitude and angle values for the amplitudes of the combined pathways (0), $(\epsilon_1^+) + (\epsilon_1^-)$, and $(\epsilon_2^+) + (\epsilon_2^-)$ are presented in Table 2.

Table 2 Composite pathway magnitudes and relative angles for the numerical solution and the true solution

Pathway amplitude	Numerical solution	True solution	Numerical solution	True solution
	Magnitude		Angle (cosine)	
$U_{ba}^0(0)$	0.2356	0.2356	1	1
$U_{ba}^1(\epsilon_1^+) + U_{ba}^1(\epsilon_1^-)$	0.8583	0.8583	0.1642	0.1642
$U_{ba}^1(\epsilon_2^+) + U_{ba}^1(\epsilon_2^-)$	0.3856	0.3856	0.0445	0.0445

The magnitude and cosine of the angle relative to the $U_{ba}^0(0)$ pathway amplitude are printed instead of the complex valued amplitudes themselves. The magnitudes and relative angles are invariant to overall phase, so no corrective alignment is needed as in Table 1

7 Some specific cases

Given a specific system of quadratic equations, algorithmic methods, such as Gröbner Basis techniques, could be used to simultaneously establish uniqueness and construct the solution [18–20]. The computational complexity of these methods render them impractical in this setting where the number of variables involved can be large. However, in some cases the actual system of equations is considerably less involved. Often, physical knowledge of the system can eliminate a number of pathways (e.g., those representing forbidden transitions) and greatly simplify the resultant system of equations.

Systems in which either a pathway, or its conjugate pathway contribute (but not both), present a case which can be treated by an efficient algorithm. One example of a physical circumstance which leads to such a case is the rotating wave approximation (RWA), which has previously been considered in connection with illustrating HE [11]. Consider a system under AP-modulation. The effect of eliminating a pathway or its conjugate is to reduce the number of variables in the quadratic system. In the following example each pathway in which ϵ_m^- appears will have zero amplitude. In addition to reducing the dimensionality of the problem, the RWA decouples the quadratic equations in a way that essentially makes the system triangular.

Consider an example in which $N = 1$, $M = 2$, and $B = 2$. Discarding the pathway amplitudes $U_{ba}^1(\epsilon_1^-)$ and $U_{ba}^1(\epsilon_2^-)$, the remaining unknown pathway amplitudes are $U_{ba}^0(0)$, $U_{ba}^1(\epsilon_1^+)$, and $U_{ba}^1(\epsilon_2^+)$. There is one zeroth order equation

$$U_{ba}^0(0)\bar{U}_{ba}^0(0) = u_0. \tag{44}$$

We may readily solve this equation, and select the overall phase, by setting $y_0 = 0$ and $x_0 = +\sqrt{u_0}$. There are four first order equations

$$U_{ba}^0(0)\bar{U}_{ba}^1(\epsilon_1^+) = u_1 \tag{45}$$

$$U_{ba}^1(\epsilon_1^+)\bar{U}_{ba}^0(0) = \bar{u}_1 \tag{46}$$

$$U_{ba}^0(0)\bar{U}_{ba}^1(\epsilon_2^+) = u_2 \tag{47}$$

$$U_{ba}^1(\epsilon_2^+)\bar{U}_{ba}^0(0) = \bar{u}_2 \tag{48}$$

Substituting $x_0 + iy_0 = U_{ba}^0(0)$ into these equations results in a linear system of four equations in the four unknowns, $U_{ba}^1(\epsilon_m^\sigma) = x_m^\sigma + iy_m^\sigma$. This scheme can be extended for any value of N and M. At each order, every term is a product containing an unknown pathway with an already computed, lower order pathway, making all of the equations linear. This approach is not possible in the general case because the analogous linear system at each order is underdetermined.

This sequential solution approach applies to each successive order because only one new variable is introduced in each equation. However, this algorithm is limited to P- and AP-modulation with conjugate pathways removed. The elimination of certain pathways from consideration by physical reasoning is most helpful, and has been used in other HE work [14]. Following the work in [14], a discrete quantum

system with five states is considered here. A genetic algorithm was used to determine a control field which transferred the population from the first state to the fifth state ($|1\rangle \rightarrow |5\rangle$), with a total yield of 83%. The control field was built from six components, which in turn were each split into two additional components under P-modulation: $\epsilon_1^{\sigma_1}, \ldots, \epsilon_6^{\sigma_6}$. Five significant field composite pathways were determined as $(\epsilon_6^-, \epsilon_1^-)^*$, $(\epsilon_5^-, \epsilon_2^-)^*$, $(\epsilon_4^-, \epsilon_3^-)^*$, $(\epsilon_5^-, \epsilon_1^-, \epsilon_1^-)^*$ and $(\epsilon_6^-, \epsilon_2^-, \epsilon_1^+)^*$. P-modulation produced six equations in these five unknowns

$$\begin{aligned}
U_{51}^2((\epsilon_6^-, \epsilon_1^-)^*)\bar{U}_{51}^2((\epsilon_5^-, \epsilon_2^-)^*) &= 0.072 - 0.015i \\
U_{51}^2((\epsilon_5^-, \epsilon_2^-)^*)\bar{U}_{51}^2((\epsilon_4^-, \epsilon_3^-)^*) &= 0.076 + 0.036i \\
U_{51}^2((\epsilon_4^-, \epsilon_3^-)^*)\bar{U}_{51}^2((\epsilon_6^-, \epsilon_1^-)^*) &= 0.081 - 0.020i \\
U_{51}^2((\epsilon_4^-, \epsilon_3^-)^*)\bar{U}_{51}^3((\epsilon_5^-, \epsilon_1^-, \epsilon_1^-)^*) &= 0.009 - 0.037i \\
U_{51}^2((\epsilon_4^-, \epsilon_3^-)^*)\bar{U}_{51}^3((\epsilon_6^-, \epsilon_2^-, \epsilon_1^+)^*) &= 0.015 + 0.036i \\
U_{51}^3((\epsilon_6^-, \epsilon_2^-, \epsilon_1^+)^*)\bar{U}_{51}^3((\epsilon_5^-, \epsilon_1^-, \epsilon_1^-)^*) &= 0.015 - 0.002i. \qquad (49)
\end{aligned}$$

Such systems of equations are typical in HE, and are much less complex than the more general case in Sect. 6.1. This overdetermined system of equations may be solved [14], and the complex values of the pathway amplitudes are $\{U_{51}^2((\epsilon_6^-, \epsilon_1^-)^*)$, $U_{51}^2((\epsilon_5^-, \epsilon_2^-)^*)$, $U_{51}^2((\epsilon_4^-, \epsilon_3^-)^*)$, $U_{51}^3((\epsilon_5^-, \epsilon_1^-, \epsilon_1^-)^*)$, $U_{51}^3((\epsilon_6^-, \epsilon_2^-, \epsilon_1^+)^*)\}$=$\{0.270$, $0.267 + 0.055i$, $0.300 - 0.047i$, $0.000 - 0.123i$, $0.024 - 0.121i\}$. The pathways associated with these amplitudes account for a yield of about 80%, which is close to the overall yield of 83%.

The overall phase was selected by setting the amplitude $U^2(\epsilon_6^-, \epsilon_1^-)^*$ to be real and positive. A physically motivated choice between solutions related by reflection symmetry was made. However, the form of $|U_{51}(s)|^2$ could also have been attributed to a mechanism consisting of the conjugate composite pathways $(\epsilon_6^+, \epsilon_1^+)^*$, $(\epsilon_5^+, \epsilon_2^+)^*$, $(\epsilon_4^+, \epsilon_3^+)^*$, $(\epsilon_5^+, \epsilon_1^+, \epsilon_1^+)^*$ and $(\epsilon_6^+, \epsilon_2^+, \epsilon_1^-)^*$. The set of amplitudes would then have been $\{0.270, 0.267 - 0.055i, 0.300 + 0.047i, 0.000 + 0.123i, 0.024 + 0.121i\}$.

8 Conclusions

This paper considers some fundamental issues occurring in mechanism extraction from observable quantum control data. As a result of the quadratic nature of observables in quantum mechanics, two fundamental symmetries arise due to the global phase and reflection. In general the number of equations obtained through the process of encoding is much larger than the number of variables to be extracted. Therefore, it is unlikely that multiple solutions exist, except those which are related to each other by simple symmetries.

It is necessary to address the validity of the assumptions made about the laboratory setting in order to realize HE experimentally. One significant idealized assumption is that the observed data is free of noise, which will not be the case in the laboratory. Noisy data will likely create an inconsistent system of equations. A solution in this context will then mean a set of pathway amplitudes which minimizes the mean square

error in the equations. An analysis of the impact of noise on mechanism determination may be found in [13,14].

Another major assumption is that any proposed modulation scheme can be realized experimentally. In practice there will be a limit on the amount of information that can be reliably encoded into the field by the pulse shaper. For example, there will be limitations on the values of the functions $g(s)$. An experimental setup that uses an 8-bit controller for phase can divide the range $[0, 2\pi]$ into 256 intervals. This will limit the resolution of the modulation functions over s, and therefore the quality of pathway amplitudes that can be extracted. Realistic laboratory conditions can limit the accuracy of the derived mechanisms; these issues are practical considerations, but not fundamental barriers to employing HE. This paper shows that the basis of HE is well defined and that future applications of HE in the laboratory may be approached with an assurance on the foundations of the technique.

Acknowledgments The authors acknowledge support from DOE.

Appendix

This appendix derives the formulas which appear in Sect. 5. Pathway amplitudes are each identified by unique s-functions which arise during modulation. In Sect. 5 exponential functions were used to construct the composite s-functions, and we may count the number of unique exponents created by modulation in order to count pathways. The exponents themselves are sums (not products), and thus the counting problem reduces to counting the number of unique ways to achieve these sums up to the underlying order N for the variables, and up to the observed order B for the equations. In particular, each exponent that it is possible to create from the s-functions will correspond to an actual pathway amplitude or product of pathway amplitudes. Each exponent is a linear combination of the modulating coefficients with integer coefficients. For example, the pathway $(\epsilon_1, \epsilon_2, \epsilon_1)$ under A-modulation corresponds to the modulation exponent $2\alpha_1 + \alpha_2$. Let the order of the exponent be the same as the order of the pathway, which is three in this example. For a given order n, the number of ways to produce a unique exponent is related to the number of ways to choose n modulating coefficients, with replacement, from the set of all available coefficients.

A-modulation

The real and imaginary components of each pathway amplitude are treated as two separate real variables. The total number of variables is equal to twice the number of pathways of all orders from 0 to N. To count the number of contributing pathways of order $n \in \{0, N\}$, consider the combinatorial problem of distributing n identical balls in M bins, where M is the number of field components available for modulation. A ball placed in the mth bin represents one contribution of ϵ_m to the pathway. The problem reduces to choosing n objects, with replacement, from M, and the solution is

$\binom{M-1+n}{M-1}$. Summing over all orders n and multiplying by 2 (to account for real and imaginary parts) gives the number of variables

$$v = 2\sum_{n=0}^{N}\binom{M-1+n}{M-1}, \tag{A.1}$$

which is Eq. 30.

For each $b \in \{0, \ldots, B\}$ there will be a single equation for each unique exponent of order b. The equations are not split into real and imaginary parts as the variables were, and there are two reasons for this choice. First, some of the equations are strictly real, and the imaginary part would yield only the trivial equation $0 = 0$. Second, the conjugate of each equation is itself one of the equations that will appear, and conjugate equations are independent. As with the number of variables, the number of equations at a given observed order b, is equivalent to filling M bins with b balls, with replacement. The total number of equations from A-modulation is

$$e = \sum_{b=0}^{B}\binom{M-1+b}{M-1}, \tag{A.2}$$

which is Eq. 31.

To show that the extremal cases produce overdetermined systems, first let $B = 2N$. The inequality $\binom{a+t}{a} < \binom{a+t+\tau}{a}$ (assuming $a > 0$ and $\tau > 0$) shows that

$$2\sum_{t=0}^{T}\binom{a+t}{a} < \sum_{t=0}^{2T}\binom{a+t}{a}, \tag{A.3}$$

and thus the system is overdetermined.

For the case $B = N + 1$, first note that for $T(T+1) < a$,

$$(T+1)\frac{(a+T)!}{T!a!} < \frac{(a+T+1)!}{(T+1)!a!}, \tag{A.4}$$

so

$$\sum_{t=0}^{T}\binom{a+t}{a} < (T+1)\binom{a+T}{a} < \binom{a+T+1}{a}, \tag{A.5}$$

therefore

$$2\sum_{t=0}^{T}\binom{a+t}{a} = \sum_{t=0}^{T}\binom{a+t}{a} + \sum_{t=0}^{T}\binom{a+t}{a} \tag{A.6}$$

$$< \sum_{t=0}^{T} \binom{a+t}{a} + \binom{a+T+1}{a} \tag{A.7}$$

$$= \sum_{t=0}^{T+1} \binom{a+t}{a} \tag{A.8}$$

If we replace a by $M-1$, and T by N then for $N(N+1) < M-1$ or

$$N^2 + N + 1 < M, \tag{A.9}$$

then the system is shown to be overdetermined.

AP-modulation

The case of AP-modulation is nearly identical to that of A-modulation. The difference is that the number of field components is effectively doubled by splitting ϵ_m into ϵ_m^+ and ϵ_m^-. The remaining arguments are analogous to the A-modulation case.

P-modulation

P-modulation presents a new challenge because pathway classes, not individual pathways are the objects of interest. Again, imagining balls being placed in bins, the new features in the problem occur when a pair of bins corresponding to ϵ_m^+ and ϵ_m^- are both filled. The P-modulation pathway classes refer only to net interactions with field components, and contributions to ϵ_m^+ and ϵ_m^- cancel with each other. These pairs of bins must be grouped together because they cannot both be filled, so only up to M field components out of the $2M$ total components may be chosen simultaneously.

The cases of zero or one ball (1 and $2M$ configurations, respectively) do not present any pairing problems, so these two terms are collected and written separately $(1+2M)$. Now consider M bins, where bin m represents either ϵ_m^+ or ϵ_m^-. If there are $t \geq 2$ balls, consider the case that exactly k bins are filled with the t balls. There are $\binom{M}{k}$ ways to pick k bins, and $\binom{k-1+(t-k)}{k-1} = \binom{t-1}{k-1}$ ways to fill them such that at least one ball is in each bin. Finally, since each of the k bins can represent either the $+$ or the $-$ component an extra factor of 2^k is required. The resulting expressions are

$$v = 2\left(1 + 2M + \sum_{n=2}^{N} \sum_{k=1}^{\min(M,n)} 2^k \binom{M}{k}\binom{n-1}{k-1}\right), \tag{A.10}$$

where $\min(M, n)$ ensures that ϵ_m^+ and ϵ_m^- are not simultaneously selected, and,

$$e = 1 + 2M + \sum_{b=2}^{B} \sum_{k=1}^{\min(M,b)} 2^k \binom{M}{k} \binom{b-1}{k-1}, \tag{A.11}$$

which are Eqs. 34 and 35, respectively.

The proofs that, for large M, $B = 2N$ and $B = N + 1$ are sufficient conditions for overdetermining the system requires additional consideration. First, if $M = 1$ and $B = 2N$, one has that $v = e + 1$. Consider then only $M \geq 2$. We wish to show that

$$\begin{aligned} &2\left(1 + 2M + \sum_{t=2}^{T} \sum_{k=1}^{\min(M,t)} 2^k \binom{M}{k} \binom{t-1}{k-1}\right) \\ &\quad < 1 + 2M + \sum_{t=2}^{2T} \sum_{k=1}^{\min(M,t)} 2^k \binom{M}{k} \binom{t-1}{k-1} \end{aligned} \tag{A.12}$$

or equivalently

$$\begin{aligned} &(1 + 2M) + \sum_{t=2}^{T} \sum_{k=1}^{\min(M,t)} 2^k \binom{M}{k} \binom{t-1}{k-1} \\ &\quad < \sum_{t=T+1}^{2T} \sum_{k=1}^{\min(M,t)} 2^k \binom{M}{k} \binom{t-1}{k-1}. \end{aligned} \tag{A.13}$$

After summation over k, each side of the inequality contains T terms where $1 + 2M$ is considered to be the first term on the left hand side. We will show term-by-term that the left hand side is less than the right hand side. Examine the first term on the left hand side of Eq. A.13,

$$\begin{aligned} 1 + 2M &< \min(M, T + 1)2M \\ &< \min(M, T + 1)\left(2^1 \binom{M}{1} \binom{T}{0}\right) \\ &< \sum_{k=1}^{\min(M,T+1)} 2^k \binom{M}{k} \binom{T}{k-1}. \end{aligned}$$

Now compare general terms corresponding to $t = t' > 0$,

$$\begin{aligned} \binom{t'-1}{k-1} &< \binom{T+1+t'-1}{k-1} \\ \sum_{k=1}^{\min(M,t')} 2^k \binom{M}{k} \binom{t'-1}{k-1} &< \sum_{k=1}^{\min(M,T+1+t')} 2^k \binom{M}{k} \binom{T+1+t'-1}{k-1}. \end{aligned}$$

To show that $B = N + 1$ is sufficient to ensure an overdetermined system in the limit of large M, begin with the following inequality

$$(T+1)!\frac{(M-(T+1))!}{(M-2)!}\frac{1+2M}{M(M-1)} + C\frac{(T+1)}{(M-T)} < 1. \tag{A.14}$$

To see this, hold T and C constant, then both terms on the left hand side may be made as small as desired by increasing M. After some manipulation the inequality becomes

$$\frac{(T+1)!(M-(T+1))!}{M!}(1+2M) + C\frac{(T+1)!(M-(T+1))!}{T!(M-T)!} < 1. \tag{A.15}$$

Now multiply both sides by $\binom{M}{(T+1)}$ and replace C with $T2^T(u_1 - u_2)$.

$$\begin{aligned}
(1+2M) + T2^T(u_1-u_2)\binom{M}{T} &< \binom{M}{T+1} \\
(1+2M) + \sum_{k=1}^{T} 2^k(u_1-u_2)\binom{M}{T} &< 2^{T+1}\binom{M}{T+1} \\
(1+2M) + \sum_{k=1}^{T} 2^k\binom{M}{k}u_1 &< 2^{T+1}\binom{M}{T+1} + \sum_{k=1}^{T} 2^k\binom{M}{k}u_2.
\end{aligned} \tag{A.16}$$

Let $u_1 = \sum_{t=2}^{T}\binom{t-1}{k-1}$ and $u_2 = \binom{T}{k-1}$

$$(1+2M) + \sum_{k=1}^{T} 2^k\binom{M}{k}\sum_{t=2}^{T}\binom{t-1}{k-1} < \sum_{k=1}^{T+1} 2^k\binom{M}{k}\binom{T}{k-1} \tag{A.17}$$

$$(1+2M) + \sum_{t=2}^{T}\sum_{k=1}^{t} 2^k\binom{M}{k}\binom{t-1}{k-1} < \sum_{k=1}^{T+1} 2^k\binom{M}{k}\binom{T}{k-1}. \tag{A.18}$$

Since M may be arbitrarily large and t is bounded, one may choose M large enough so that $\min(M,t) = t$. This makes the left and right hand sides of Eq. A.18 equivalent to the original expressions for the number of variables and equations, respectively. That is, for large M

$$(1+2M) + \sum_{t=2}^{T}\sum_{k=1}^{\min(M,t)} 2^k\binom{M}{k}\binom{t-1}{k-1} < \sum_{t=T+1}^{T+1}\sum_{k=1}^{\min(M,t)} 2^k\binom{M}{k}\binom{t-1}{k-1}, \tag{A.19}$$

and therefore

$$2\left((1+2M)+\sum_{t=2}^{T}\sum_{k=1}^{\min(M,t)}2^k\binom{M}{k}\binom{t-1}{k-1}\right)$$
$$<(1+2M)+\sum_{t=2}^{T+1}\sum_{k=1}^{\min(M,t)}2^k\binom{M}{k}\binom{t-1}{k-1}. \tag{A.20}$$

For all three modulation schemes, HE can produce an overdetermined system of equations. Overdetermined systems will generally support multiple solutions in cases where the equations themselves are related, such as by symmetry.

References

1. R.S. Judson, H. Rabitz, Phys. Rev. Lett. **68**, 1500 (1992)
2. W.S. Warren, H. Rabitz, M. Dahleh, Science **259**, 1581 (1993)
3. A. Assion, T. Baumert, M. Bergt, T. Brixner, B. Kiefer, V. Seyfried, M. Strehle, G. Gerber, Science **282**, 919 (1998)
4. R.J. Levis, G.M. Menkir, H. Rabitz, Science **292**, 709 (2001)
5. T. Feuer, A. Glass, T. Rozgonyi, R. Sauerberg, G. Szabo, Chem. Phys. **267**, 223 (2001)
6. S. Vajda, A. Bartelt, E.C. Kaposta, T. Leisner, C. Lupulescu, S. Minemoto, P. Rosendo-Francisco, L. Woste, Chem. Phys. **267**, 231 (2001)
7. D. Meshulach, Y. Silberberg, Nature **396**, 239 (1998)
8. T.C. Weinacht, J. Ahn, P.H. Bucksbaum, Nature **397**, 233 (1999)
9. R. Bartels, S. Backus, E. Zeek, L. Misoguti, G. Vdovin, I.P. Christov, M.M. Murnane, H. Kapteyn, Nature **406**, 164 (2000)
10. T. Hornung, R. Meier, M. Motzkus, Chem. Phys. Lett. **326**, 445 (2000)
11. A. Mitra, H. Rabitz, Phys. Rev. A **67**, 033407 (2003)
12. R.W. Sharp, H. Rabitz, J. Chem. Phys. **121**, 4516 (2004)
13. A. Mitra, H. Rabitz, J. Chem. Phys. **125**, 194107 (2006)
14. A. Mitra, H. Rabitz (to be published)
15. A. Mitra, I. Solá, H. Rabitz, Phys. Rev. A **67**, 043409 (2003)
16. A. Mitra, H. Rabitz, J. Phys. Chem. A **108**, 4778 (2004)
17. O.F. Aliş, H. Rabitz, M.Q. Phan, C. Rosenthal, M. Pence, J. Math. Chem. **35**, 65 (2004)
18. D. Kapur, Y.N. Lakshman, in *Symbolic and Numerical Computation for Artificial Intelligence*, ed. by B. Donald, D. Kapur, J. Mundy (AP, 1992) pp. 45–87
19. B. Buchberger, in: *Gröbner Bases and Applications*, ed. by B. Buchberger, F. Winkler (CUP, 1998) pp. 3–31
20. B. Buchberger, in: *Gröbner Bases and Applications*, ed. by B. Buchberger, F. Winkler (CUP, 1998) pp. 535–545